R/F

The Role of Tomosynthesis Imaging at Our Institute and X-ray Dose Optimization

Tetsuta Izumi R.T.

Osaka International Cancer Institute, Diagnostic and Interventional Radiology Section[1]
Osaka International Cancer Institute, Orthopedic Surgery (Musculoskeletal Oncology) and Rehabilitation Section[2]
Tetsuta Izumi[1], Ayano Sakamoto[1], Minoru Kawamata[1], Yasuhiko Yamane[1], Akitoshi Yoneda[1], Hideaki Okamoto[1], Kazuya Oshima[2], Katsuyuki Nakanishi[1]

1. Introduction to Osaka International Cancer Institute

In March of last year (2017), Osaka Medical Center for Cancer and Cardiovascular Diseases changed its name to Osaka International Cancer Institute and reopened as a new hospital in Otemae, Chuo-ku, Osaka **(Fig. 1)**. The institute has 500 beds, 35 medical departments, 13 floors above ground, 2 floors below ground, and a total floor area of approx. 68,000 m^2, an increase of approx. 10,000 m^2 from the previous site. The institute is located adjacent to Osaka Castle and a spectacular view of the castle can be enjoyed from the hospital wards **(Fig. 2)**. The institute is designated an advanced treatment hospital and prefectural core hospital for cancer care by the Japanese Ministry of Health, Labor and Welfare, and as well as providing specialist cancer care, it is also responsible for maintaining a cooperative system for cancer care provision and provides cancer-related counseling and support in Osaka Prefecture.

The core principle of the institute is expressed by the motto “provision and development of advanced patient-based cancer care.” The Diagnostic and Interventional Radiology Section of the institute to which the author is affiliated provides the latest medical care and technology to patients in a fast-evolving field.

Fig.1 Osaka International Cancer Institute

Fig.2 Osaka Castle Visible from Hospital Ward

2. Role of Tomosynthesis Imaging in the Orthopedic Surgery (Musculoskeletal Oncology) Field

According to the Cancer Information Service of National Cancer Center Japan, in 2013 there were 862,452 newly diagnosed cases of cancer. In 2015, 370,346 people died of cancer, 1 in 2 Japanese citizens developed cancer, and 1 in 3 died of cancer (Cancer Information Service, National Cancer Center Japan “Latest Cancer Statistics” (http://ganjoho.jp/reg_stat/statistics/stat/summary.html). It would not be out of place to call cancer a national affliction of the Japanese people.

The Orthopedic Surgery (Musculoskeletal Oncology)

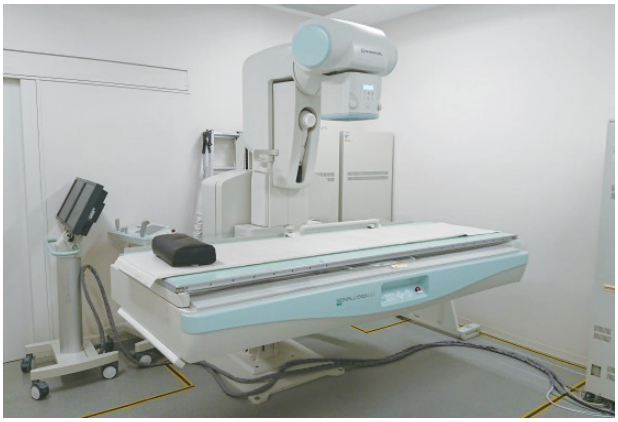

Fig.3 SONIALVISION G4 in the Institute

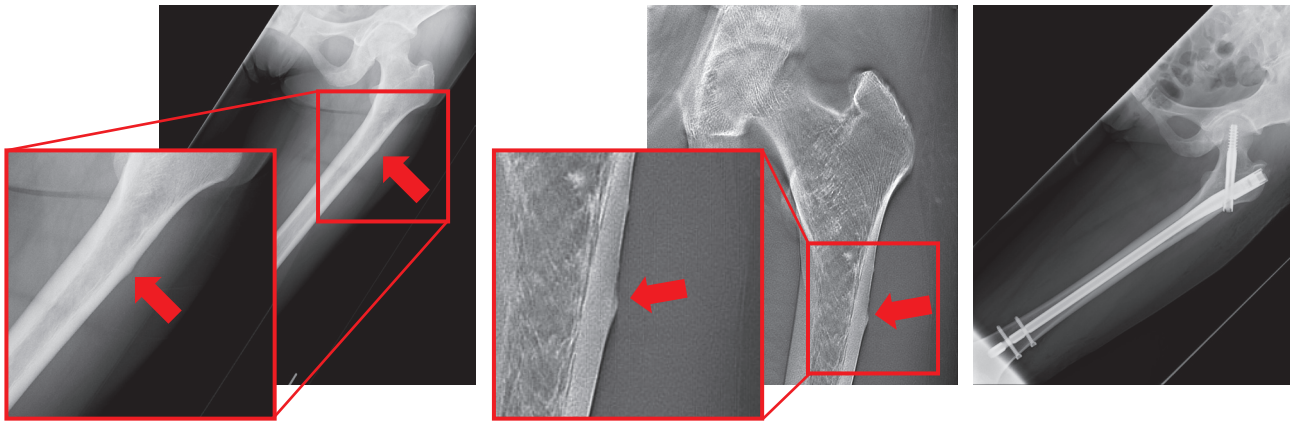

Fig.4 Care of AFF with Gamma Nails Inserted
(Left) Radiographs, (Middle) Tomosynthesis Images, (Right) Postoperative Radiograph

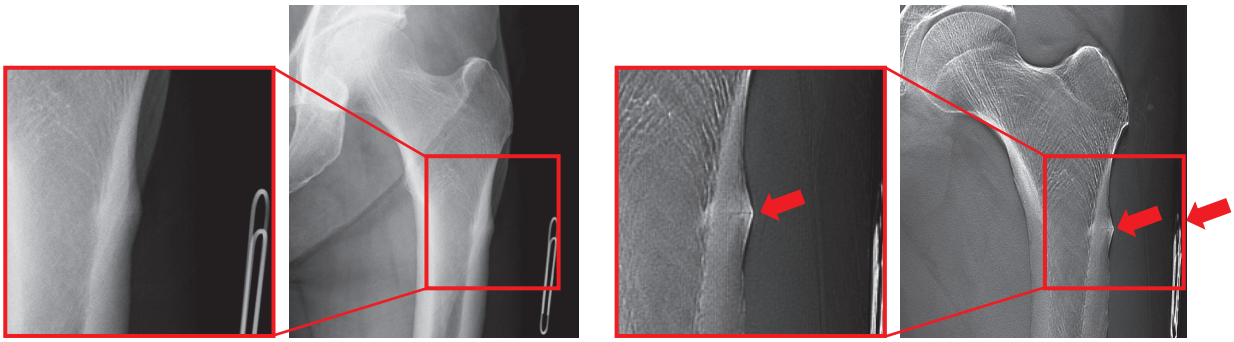

Fig.5 Image Verification of AFF and Marker Position
(Left) Radiographs, (Right) Tomosynthesis Images

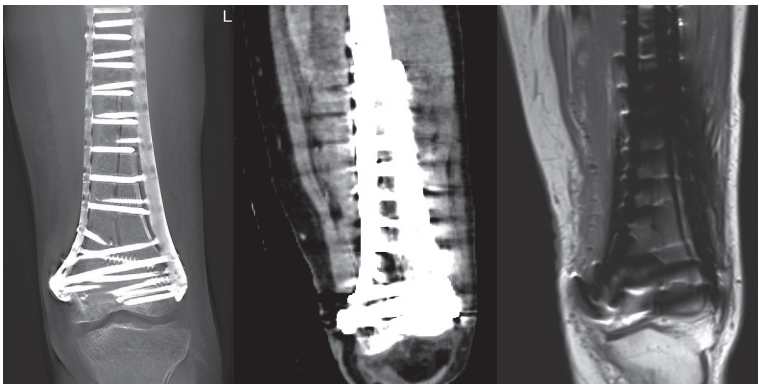

Fig.6 Images After Musculoskeletal Tumor Surgery
(Left) Tomosynthesis Image, (Middle) CT-MPR Image, (Right) MRI-T1 weighted Image

Section mainly handles patients with musculoskeletal tumors, and carries out tomosynthesis imaging with SONIALVISION G4 **(Fig. 3)** for diagnosis, treatment, and follow-up observations of musculoskeletal tumors and metastatic bone tumors. This article describes cases in which tomosynthesis imaging was found to be useful.

In a case of atypical femoral fracture (AFF) associated with bone metastasis of breast cancer **(Fig. 4)**, minute bulging of the bone cortex could barely be seen in radiographs, but the fracture line inside the bone cortex bulge was clearly visible in tomosynthesis images after the section height was matched to the bulge. Surgical operation was chosen to maintain patient QOL due to risk of fracture, and Gamma nails were inserted as preventive treatment.

In the next case of AFF **(Fig. 5)**, the fracture line was clearly visible with tomosynthesis imaging just as was seen in **Fig. 4**. In order to use a low-intensity pulsed ultrasound (LIPUS) fracture healing system that shortens bone union times by close to 40 %, radiography and tomosynthesis imaging were performed with a paper clip as a marker. Compared to radiographs, tomosynthesis images allowed the section depth to be matched to the fracture line and determination of depth from the skin surface.

Fig. 6 shows images after surgery for a musculoskeletal tumor. Tumor-affected bone was removed together with the tumor, residual tumor cells were killed completely by direct irradiation, and the bone

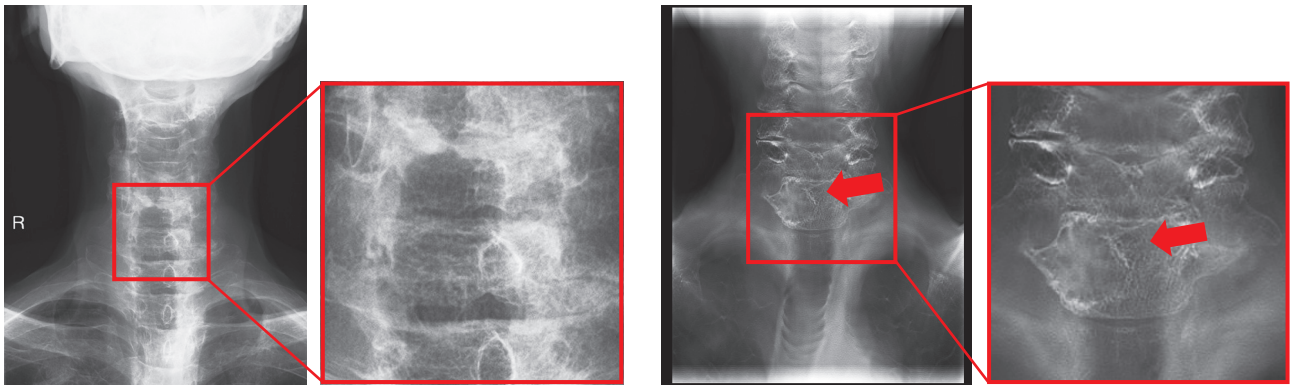

Fig.7 Images of Osteolytic Spinal Metastasis of Renal Cancer
(Left) Radiographs, (Right) Tomosynthesis Images

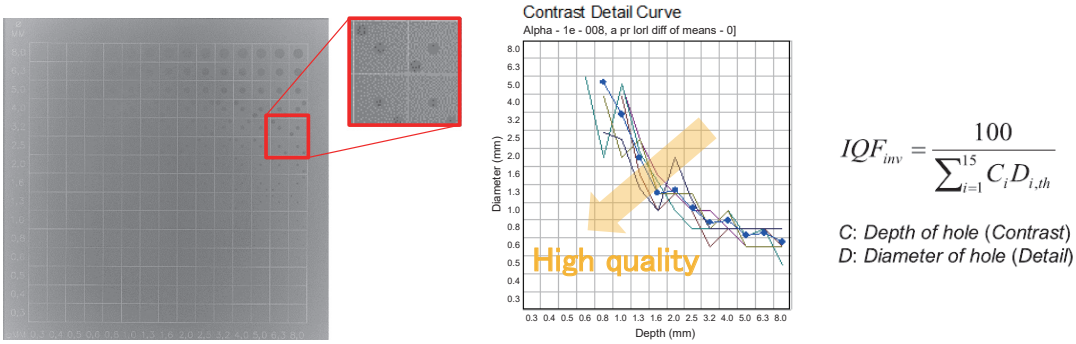

Fig.8 CD Curve and IQF inv. Calculated by CDRAD Analyser

was returned to the body and fixed with metal (intraoperative extracorporeal autogenous irradiated bone graft surgery). Postoperative follow-up was required to observe bone union, but CT examinations could not be used due to metal artifacts from high absorption materials, and MRI examinations could not be used due to magnetic susceptibility artifacts caused by the metal. Meanwhile, reconstruction of tomosynthesis images with T-smart (Tomosynthesis-Shimadzu Metal Artifact Reduction Technology) produces images with few visible artifacts around metal objects and made it possible to observation bone union in follow-up.

Tomosynthesis imaging was also useful in a case of renal cancer with osteolytic spinal metastasis **(Fig. 7)**. Identifying the lesion area was difficult with radiography, but after matching the section height, the lesion area was well-visualized on tomosynthesis images.

As described earlier, tomosynthesis images are excellent for observing bone union around metal materials and intraosseous changes that are difficult to observe with radiography, CT and MR. Tomosynthesis imaging is also quicker and simpler to perform compared to CT and MR and produces a lower X-ray dose than CT, which is why tomosynthesis imaging is being used more and more often at our institute.

3. Evaluation of Tomosynthesis Image Quality

The previous section mentioned that tomosynthesis has a very high detection capability compared to radiography. We performed an experiment to compare the difference in detection capability between tomosynthesis and other imaging modalities. Signal detection capability was tested using an Artinis Medical System CDRAD phantom and CDRAD Analyser V1.1 analysis software from the same company, which carried out calculations automatically. As shown in **Fig. 8**, the CDRAD phantom consists of PMMA with cells in a grid pattern, where each cell contains one hole in the middle and one hole in the corner of the cell and the diameter and depth of these holes differ between each cell. CDRAD phantom visibility is assessed using the CDRAD Analyser V1.1 software to determine the position of each hole throughout the grid pattern, draw a CD curve, and calculate IQF inv. as a quantitative indicator of image quality. The software calculates the CD curve automatically, so results can be calculated easily. IQF inv. calculated using the equation shown in **Fig. 8** is a quantitative indicator of overall image quality that incorporates image contrast and graininess, where higher IQF inv. represents better image quality and shows visualization of small, low-contrast signals.

This experiment simulated musculoskeletal imaging by placing the CDRAD phantom in the middle of 20 cm of PMMA **(Fig. 9)** and performing radiography and tomosynthesis imaging 5 times each. Radiography imaging conditions were tube voltage: 75 kV, tube current-time product: 16 mAs, and tomosynthesis imaging conditions were tube voltage: 80 kV, tube current-time product: 2.5 mAs, and tomography swing angle: 40°. Iterative reconstruction (T-smart) was the image reconstruction method used for tomosynthesis imaging, and image reconstruction was only performed for one central image. The mean results from 5 acquisitions and an expanded view of part of the rendered images are shown in **Fig. 10**. Under even gross examination, the ability for tomosynthesis to detect holes in the cells is clearly greater than in radiographs. In addition, IQF inv. also shows the greater detection capability of tomosynthesis images (6.33) compared to radiographs (4.47).

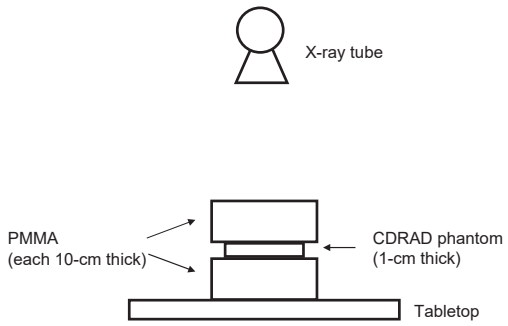

Fig.9

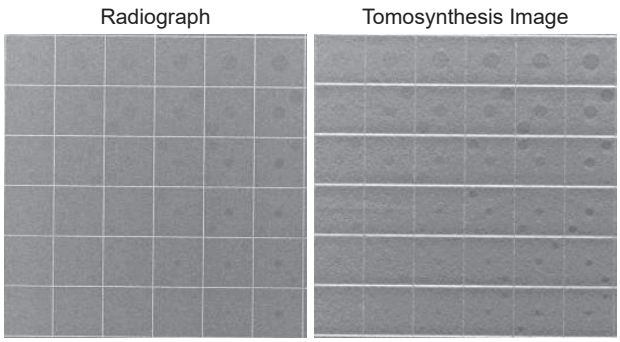

IQF inv. **4.47** **6.33**

Fig.10 CDRAD Phantom Images and IQF inv.

4. Reducing the X-ray Dose of Tomosynthesis

Orders for tomosynthesis images in the field of orthopedics at our institute are often for follow-up observations and images from 2 directions, and are often ordered alongside other imaging modalities (including radiography). As a consequence, we need to take measures to reduce the X-ray dose of tomosynthesis imaging. We looked to the accessory filters built into SONIALVISION G4 as a means of reducing X-ray dose. A Cu 0.1 mm filter is selected by manufacturer-recommended imaging conditions, but the user can change this to Cu 0.2 mm and Cu 0.3 mm filters **(Fig. 11)**. Making the accessory filter thicker can exclude the soft X-ray component, but also reduce the quantity of X-rays that reach the FPD and produce noise throughout the image. We investigated whether it was possible to maintain image quality while reducing the X-ray dose by increasing the accessory filter thickness while reducing the additional noise component using noise reduction processing **(Fig. 12)**.

A CDRAD phantom held in the middle of 20 cm of PMMA, as shown in **Fig. 9**, was used as the imaging subject. Imaging was performed 10 times each with Cu 0.1 mm and Cu 0.2 mm accessory filters, then noise reduction processing was applied to images obtained using the Cu 0.2 mm filter to create processed images (Cu 0.2 mm (+)). OTHERS was used for noise reduction processing. Standard deviation, contrast, and CNR were calculated for background and the deepest and largest hole in the grid pattern **(Fig. 13)** from images acquired with a Cu 0.1 mm, Cu 0.2 mm, and Cu 0.2 mm (+) accessory filter. These results were tested for significant difference using the Tukey method and a 5 % significance level. CNR was calculated using the following equation.

$$CNR = \frac{\text{Contrast}}{\text{Noise}} = \frac{(\text{Mean M}/\text{Mean B})}{\text{SD B}}$$

Mean: Average of digital values SD: Standard deviation

Results are shown in **Fig. 14**. Compared to Cu 0.1 mm, standard deviation was significantly greater using Cu 0.2 mm but there was no significant difference in using Cu 0.2 mm (+). Comparing contrast against Cu 0.1 mm, Cu 0.2 mm was equivalent and Cu 0.2 mm (+) was significantly lower. Comparing CNR against Cu 0.1 mm, Cu 0.2 mm was significantly lower and Cu 0.2 mm (+) was not significantly different. Based on these results, CNR indicates that equivalent image quality to the Cu 0.1 mm filter used by default imaging conditions can be obtained

Fig.11 Accessory Filter Thickness Adjustment Windows

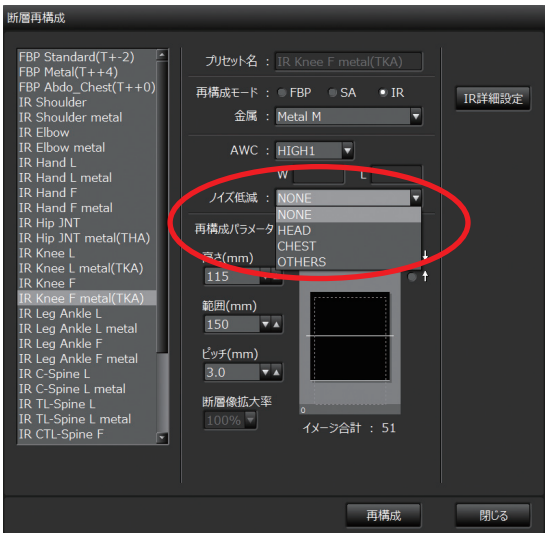

Fig.12 Noise Reduction Processing

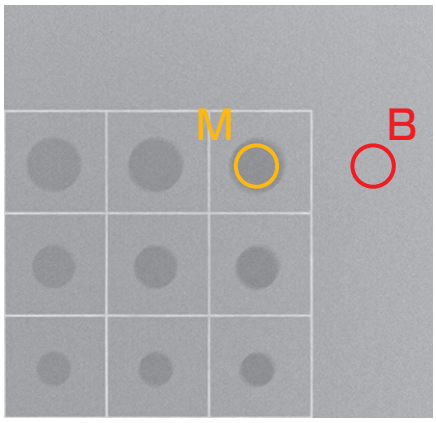

Fig.13 Standard Deviation, Contrast, and CNR Measurements

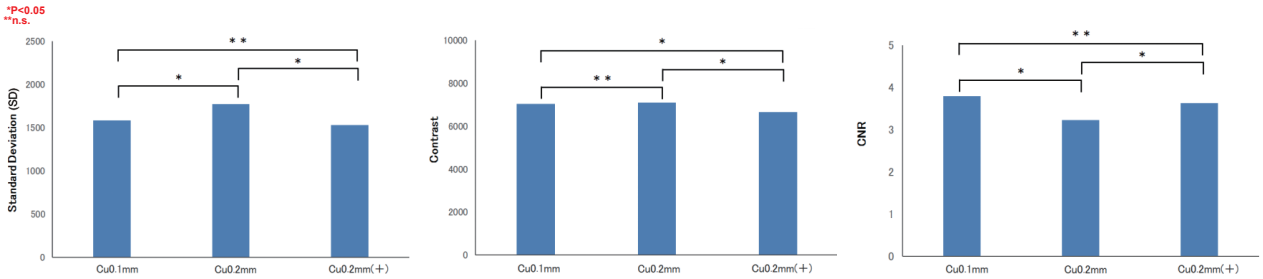

Fig.14 Standard Deviation, Contrast, and CNR Results

by changing to the Cu 0.2 mm accessory filter and applying noise reduction processing. Noise reduction processing reduced image contrast, but this can be resolved using the digital characteristics of the image and adjusting WW/WL. **Fig. 15** shows the tomosynthesis images of a pelvis phantom. There appears to be no major difference between the Cu 0.1 mm image and the Cu 0.2 mm (+) image.

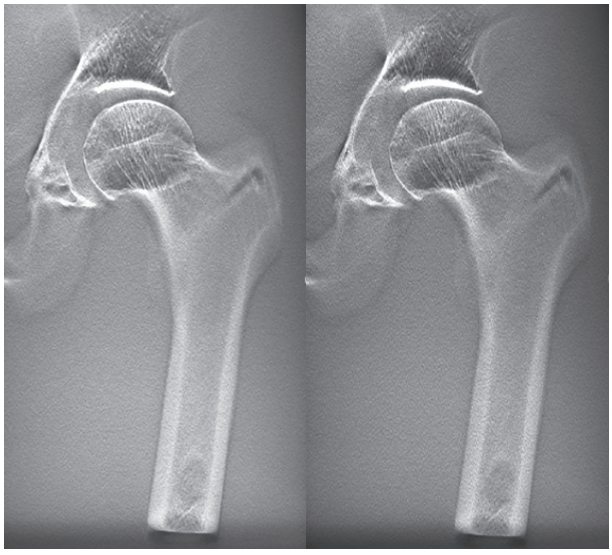

Fig.15 Images of Pelvis Phantom
(Left) Cu 0.1 mm, (Right) Cu 0.2 mm (+)

Based on ion-chamber dosimeter measurements, this method was able to reduce the X-ray dose by approx. 30 %. This investigation was reported at the 61st Annual Meeting of the Japanese Society of Radiological Technology Kinki Branch.

5. Conclusions

Tomosynthesis examinations were useful in cases with bone tumor, atypical femoral fracture, and metal implants, and could produce information not detectable by radiography, CT, or MR. Detection of small lesions enables treatment strategy selection and can reduce the risk of fracture. X-ray dose can also be reduced while maintaining image quality by using an accessory filter with noise reduction processing. Japan Network for Research and Information on Medical Exposures (J-RIME) has published diagnostic reference levels (DRLs 2015) and there is increasing interest in X-ray doses. As radiological technologists, we look forward to making further contributions towards reducing patient X-ray doses with the help of equipment manufacturers.